

# Parametric Experimentation of Output Efficiency of Vibration-Based Impact Mode Piezoelectric Power Generator

Mohammad Faisal Afifi Mohd Daud<sup>1</sup>, Amat Amir Basari<sup>1\*</sup>, Ng Xue Yan<sup>1</sup>, Nur Amalina Ahmad Nawir<sup>1</sup>, Seiji Hashimoto<sup>2</sup>, Ahmad Sadhiqin Ahmad Isira<sup>1</sup>

<sup>1</sup>Centre for Telecommunication Research & Innovation (CeTRI), Fakulti Kejuruteraan Elektronik & Kejuruteraan Komputer (FKEKK), Universiti Teknikal Malaysia Melaka, Durian Tunggal, Melaka, 76100, MALAYSIA

<sup>2</sup>Division of Electronics and Informatics, School of Science and Technology, Gunma University, Tenjin-cho, Kiryu City, Gunma, 376-8515, JAPAN

\*Corresponding Author

DOI: <https://doi.org/10.30880/ijie.2021.13.02.008>

Received 9 June 2020; Accepted 1 December 2020; Available online 28 February 2021

**Abstract:** This paper evaluates the output efficiency and the frequency responses of a designed vibration-based impact mode piezoelectric power generator with additional interfaced plate. Indirect impact towards the piezoelectric disc is generated by sandwiching the interfaced plate between the piezoelectric disc and contact structure. The impact force can be varied by altering the bending stress of the beam. The output efficiency of the piezoelectric disc is found to increase about 87% by utilizing 1mm thickness of the vibrating beam compared to 2mm thickness. The output efficiency with the additional interfaced plate can harvest about 3 times higher than that of without the interfaced plate. In order to investigate the influence of the interfaced plate, two variables such as the interfaced plate's diameter and height are studied. It is confirmed from the experimental results that the output of the piezoelectric disc is to be inversely proportional to the height and also to the diameter of the interfaced plate.

**Keywords:** Piezoelectric, impact mode, vibration, interfaced plate

## 1. Introduction

Nowadays, the Industry Revolution 4.0 which is among of them are the adoption of wireless sensor network (WSN) is a popular trend. However, there is a struggle because of the battery limited lifespan and the replacement or rechargeable battery for that WSN nodes [1]–[3]. Thus, the ambient waste energy is scavenged so that it can be utilized to obtain the electrical energy. There are many assortments of the ambient sources namely thermal sources, solar sources, human motion, mechanical sources, acoustic energy and vibrational energy [2], [4]. The small-scale system can be powered by clean and regenerative energy which is harvested from the ambient sources [4]–[5].

Piezoelectric, electromagnetic, electrostatic and magnetostriction are varieties of the vibration energy harvester's transducer that can be applied for the energy conversion [4]–[7]. The energy conversion principle is the ability of a transducer to alter kinetic energy from vibration energy into electricity. The mechanical deformation of the energy harvester's structure is the principle of the kinetic energy harvesting device of piezoelectric materials.

In order to optimize the performance and output efficiency of the piezoelectric energy harvester, there are two main elements have been focused in the literatures which are the proof mass [4], [9]–[15] and the structures of the piezoelectric cantilever beam [9], [16]–[20].

As reported in [17], the frequency responses and the output performances can be affected by the thickness of the piezoelectric cantilever. The studies on the performance and the frequency response on the piezoelectric energy harvester based on the parameters of proof mass and the piezoelectric cantilever length are also expressed in [9]. These approaches are applied to the cantilever piezoelectric vibration energy harvester to enhance the output performances.

However, the output voltage of a piezoelectric cantilever through an impact technique is twenty times higher compared to the vibration or bending techniques as presented in [21]. In addition, the performance and efficiency of the impact-based piezoelectric energy harvester can be improved by numerous techniques. The approaches are discussed in [22]–[31]. These methods are applied to enhance the performance of the power generator. The additional of an interfaced plate and an indirectly contact on the piezoelectric disc is introduced in [30] and [31]. The indirect contact on the piezoelectric disc can improve the output efficiency up to 4.3 times higher than that of directly contact configuration. Yet, there is inadequate of details about the property of the parameters for the designed piezoelectric power generator.

This paper evaluates variables of the interfaced plate and demonstrates the designed piezoelectric power generator that can influence the efficiency of output of the piezoelectric through a continuous vibration experiment. Besides load resistance, other variables such as interfaced plate diameter, the vibrating beam’s width and thickness are also investigated. The investigation and verification of the variables can be utilized for the vibration-based impact mode piezoelectric energy harvester research.

**Table 1 - Structures of the designed power generator**

Structures	W x L x H (mm <sup>2</sup> )
Setting-based beam	50 x 140 x 5
Vibrating beam	10 x 80 x 1
Spacer	50 x 40 x 7

**Table 2 - Specification of the 7BB-35-3L0 piezoelectric disc**

Structure	Value
Diameter of plate	35 mm
Thickness of plate	0.30 mm
Diameter of the piezoelectric element	25 mm
Thickness of element	0.53 mm
Material of the plate	Brass
Capacitance of piezoelectric element	30.0 ± 30% nF
Resonant Impedance	200 Ω



**Fig. 1 - The interfaced plate structures with different sizes**

## 2. Methods and Materials

The structure of the power generator consists of setting-based beam, vibrating beam and spacer. The setting-based beam and spacer are made of aluminum. While the vibrating beam is made of stainless steel due to the aluminum does not have elasticity compared to the stainless steel. There is a 30mm diameter of hole is applied on the setting-based beam, the position where the piezoelectric disc is placed. When a force is applied, the hole will support the piezoelectric disc and stretch the piezoelectric disc in a maximum position. Therefore, it can extend the yielded output power from the applied force.

At the end of the vibrating beam a screw tip and a proof mass were attached to it. The diameter of the screw tip

used is 3mm. The screw tip is utilized to contact the piezoelectric disc with the aids of the proof mass. The other end of the vibrating beam is conjoined with the setting-based beam and spacer. The spacer is used as a separator for the setting-based beam and vibrating beam as an interfaced plate is situated between them. Table 1 shows the dimension of the structure of the power generator. The structures of the aluminum interfaced plates are shown in Fig. 1. The interfaced plates' diameters are varied as follows; 4mm, 6mm, 8mm, 10mm, 12mm and 14mm. While the heights for each interfaced plates' diameters are 1mm, 3mm, 5mm, 7mm and 9mm.

The piezoelectric disc of 7BB-35-3L0 is used in this research. This piezoelectric ceramic disc is an external drive type piezoelectric disc. It is fabricated by Murata Manufacturing Co., Ltd. The details are shown in Table 2.

Different vibration values of acceleration level for the electrodynamic shaker are applied on the piezoelectric power generator. Thus, the piezoelectric power generator is vibrated based on the setup acceleration level of the electrodynamic shaker. Meanwhile, the vibrating beam vibrates and hits on the piezoelectric ceramic disc and yielded an output voltage. The output of the piezoelectric disc is connected parallel to a decade resistance box. The decade resistance box which is manufactured by Cratech UK is determined as a load resistor. While for the width of the vibrating beam, it is varied to 8mm, 10mm, 12mm and 14mm. The thicknesses of the vibrating beam are set to two different value which are 1mm and 2mm. A load resistor is connected in parallel to the output of the piezoelectric disc. A digital storage oscilloscope is utilized to measure and record the output reading of the piezoelectric disc. The sampling time of the measurement is set to 10ms. Output efficiency of power generator is evaluated based on the comparison between one value of parameter to the other value of the same parameter.

### 3. Experimental Results and Discussion

#### 3.1 Load Resistance

The operating frequency of the piezoelectric disc is determined based on two conditions which are piezoelectric disc without interfaced plate and piezoelectric disc attached with an interfaced plate. The interfaced plate's diameter and height value used in this evaluation are 4mm and 5mm respectively. A 25g of proof mass is attached on one end of the vibrating beam. The dimension of the vibrating beam used, and the diameter of the screw used for impact on the piezoelectric disc are  $(10 \times 80 \times 1)\text{mm}^3$  and 3mm respectively. An acceleration level of 1g is applied on the electrodynamic shaker to supply a continuous vibration to the power generator with the output voltage is measured in open circuit condition.

Fig. 2 indicates the frequency responses of both piezoelectric disc configurations. The operating frequency bandwidth for both configurations is between 30Hz to 60Hz. When no interfaced plate is applied, the output voltage is increased progressively from  $12.4V_{\text{max}}$  at the frequency of 30Hz until  $31.7V_{\text{max}}$  at the frequency of 42Hz. Then, the output voltage is decreased gradually after 42Hz of frequency. The voltage of the piezoelectric disc with the interfaced plate is also increased slowly from the frequency of 30Hz at  $11.3V_{\text{max}}$ . This situation continues up to the frequency of 40Hz which yielded an output voltage of  $44.2V_{\text{max}}$ .

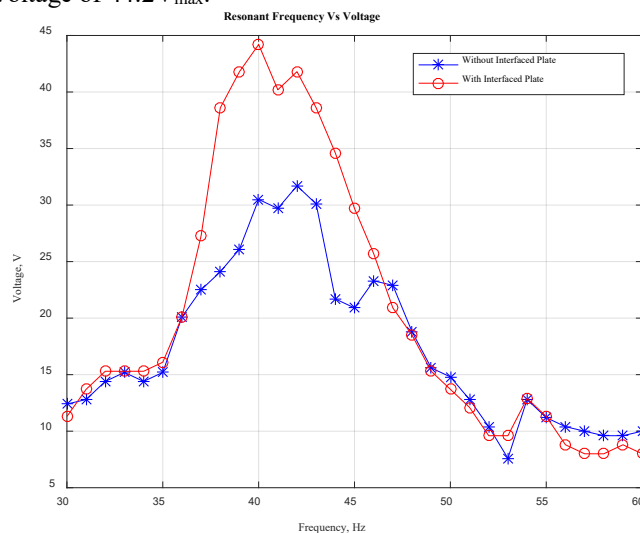
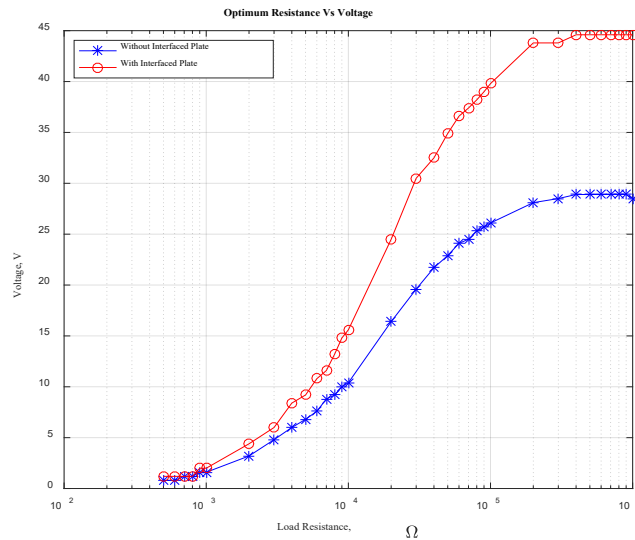


Fig. 2 - The comparison of the output voltage of both piezoelectric disc configuration



**Fig. 3 - The output voltage versus load resistance**

When the frequency is at 41Hz, the output voltage has decreased even though the frequency is continuously increased. From the same plot, it can be seen that the peaks are at 44.2V and 11.3V respectively for both with and without interfaced plate configuration. The impact energy is given by equation (1).

$$E_{imp} = E_{ei} + E_{absip1} + E_{absip2} \quad (1)$$

Equation (1) describes the total energy experienced by the piezoelectric from the impact. While  $E_{ei}$  shows the piezoelectric energy, the other two variables  $E_{absip1}$  and  $E_{absip2}$  are the energy absorbed by the interfaced plate. Meanwhile, the resonant frequency of both piezoelectric power generators configurations are 42Hz for the configuration without the interfaced plate and 40Hz for the other. The resonant frequency of an ideal spring mass system can be defined by equation (2). In this equation,  $f_0$  is the resonant frequency of the spring mass system without load, the stiffness of the piezoelectric is referred to  $k_T$  and the effective mass of the system is represented as  $m_{eff}$ .

$$f_0 = \left( \frac{1}{2\pi} \right) \sqrt{\frac{k_T}{m_{eff}}} \quad (2)$$

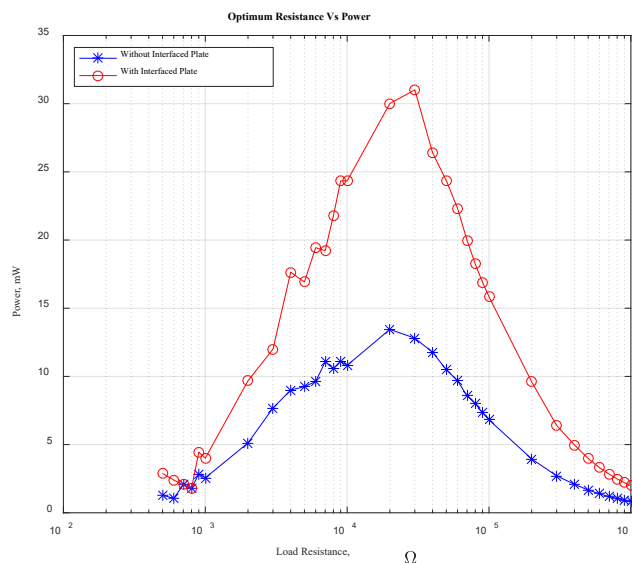


**Fig. 4 - The output power of the piezoelectric disc versus load resistance**

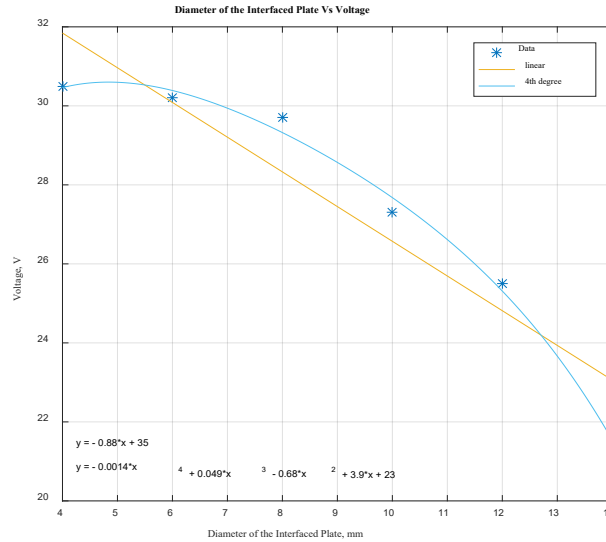


**Fig. 5 - The output voltage against diameter of interfaced plate**

After that, optimal load resistance of the piezoelectric power generator in order to harvest and obtain a peak output power is investigated. The experimental setup is same as preceding experiment except the piezoelectric output is connected to a load resistor. The output efficiency of the power generator with and without the interfaced plate is measured with the load resistance start from 500Ω to 1MΩ. Fig. 3 shows that the output voltage of the power generator is increased dramatically when the load resistance value is increased. These circumstances for both piezoelectric disc conditions are changed into saturation conditions as the resistance increased to 200kΩ. It is believed that with the assistance of the interfaced plate, the optimum contact of the screw tip is increased on the interfaced plate. Fig. 4 shows that the peak output power is at 31mW yielded when a load resistance 30kΩ is connected. Meanwhile, 13.45mW of maximum output power is generated when a 20kΩ load resistance is used.

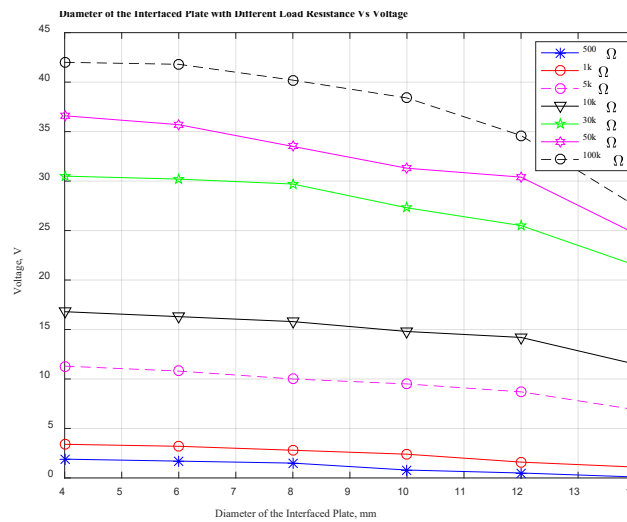


**Fig. 6 - The output voltage versus interfaced plate diameter**

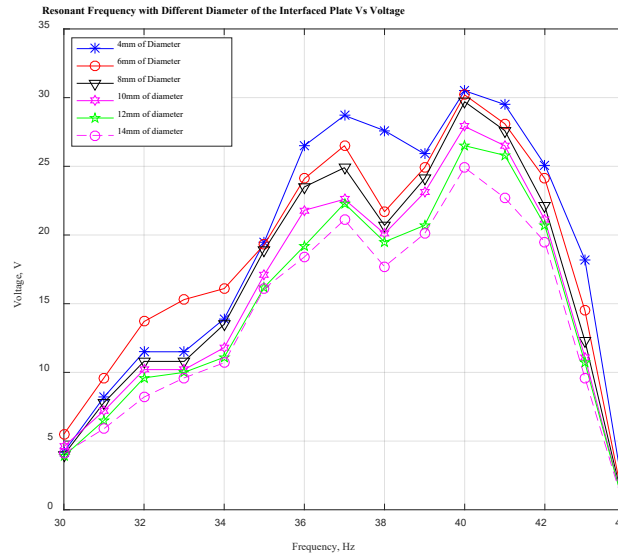


Fig. 7 - The output voltage versus the frequency with different interfaced plate diameter

### 3.2 Interfaced Plate Diameter

In order to analyse the effect of the diameter of the interfaced plate to the efficiency of the piezoelectric disc, the following experiment is executed. Proof mass used is 25g and 3mm of diameter of a screw tip is fixed on the end of the vibrating beam. The acceleration level of the electrodynamic shaker is fixed on 1g. The load resistance value of 30kΩ is connected parallel to the output terminal of the piezoelectric disc. Meanwhile, variation in the diameter of the plate is as follows; 4mm, 6mm, 8mm, 10mm, 12mm and 14mm. The plate’s height is 5mm. The result of this experiment is shown in Fig. 5. The peak output voltage value which is 30.5V<sub>max</sub> can be achieved when the interfaced plate is 4mm in diameter. Interfaced plate with longer diameter produced lower output voltage. Based on the stress equation of  $\sigma = \frac{F}{A}$ , the stress is inversely proportional to the cross-sectional area. Hence, the stress applied to the piezoelectric disc is larger with reduced diameter of the interfaced plate.

$$D_i = e_{ij}^\sigma E_j + d_{im}^d \sigma_m \quad (3)$$

Equation (3) shows the relationship of dielectric displacement of piezoelectric with the stress, where,  $D_i$  is dielectric displacement,  $E_j$  is applied electric field,  $d_{im}^d$  is piezoelectric coefficients  $e_{ij}^\sigma$  is dielectric permittivity, and  $\sigma_m$  is stress. From this equation, the dielectric displacement which also known as output voltage of the piezoelectric will increase as the stress applied to the piezoelectric disc is increased. Then, the experiment is proceeded by utilizing different value of load resistance. The load resistances are 500Ω, 1kΩ, 5kΩ, 10kΩ, 30kΩ, 50kΩ and 100kΩ. The experiment setup is same as in the previous. The diameters of the interfaced plate are 4mm, 6mm, 8mm, 10mm, 12mm and 14mm. Fig. 6 shows the result. The smaller the diameter of the interfaced plate is the higher the amplitude of the output voltage.

Next, the experiment is carried out to evaluate the frequency response of piezoelectric power generator with change in diameter of the interfaced plate. The diameters of the interfaced plate used are 4mm, 6mm and 8mm. The weight of the proof mass is 25g. The 3mm diameter of the screw tip and vibrating beam with the dimension of (10 x 80 x 1)mm<sup>3</sup> is employed. The output of the piezoelectric power generator is connected to the load resistor of 30kΩ. The graph illustrates the output voltage is shown in Fig. 7. The measurement of the frequency responses of the piezoelectric power generator is taken from 30Hz to 44Hz of frequency. The output voltage is starting to increase at the frequency is 30Hz. The resonant frequency of the three of the three interfaced plate is at 40Hz. The peak output voltage of the interfaced plates are 30.5V<sub>max</sub>, 30.2V<sub>max</sub> and 29.7V<sub>max</sub>, respectively. The output voltage of the three configured power generators are declined rapidly after the resonant frequency.

### 3.3 Vibrating Beam Stiffness

This subsection describes the effect of the stiffness of vibrating beam to the output of the power generator. Two parameters are varied. They are the width and thickness of the beam.

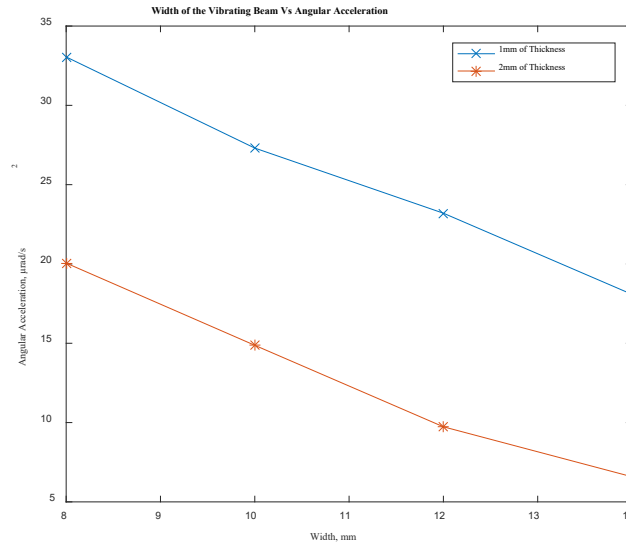


Fig. 8 - The angular acceleration versus vibrating beam with different width

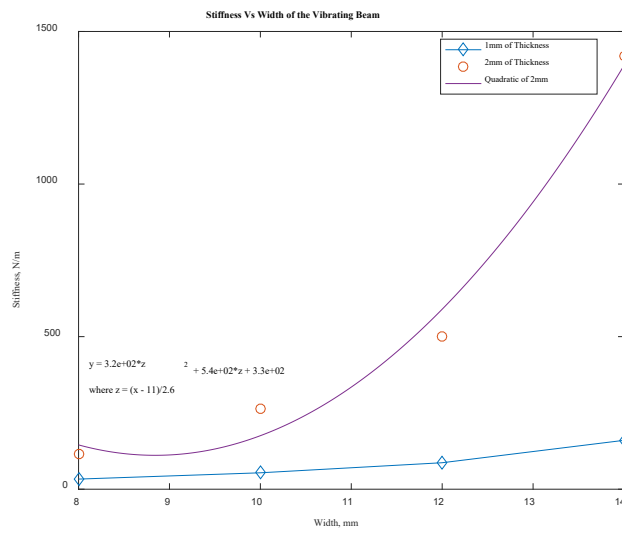


Fig. 9 - The stiffness versus the width with different thickness of the vibrating beam

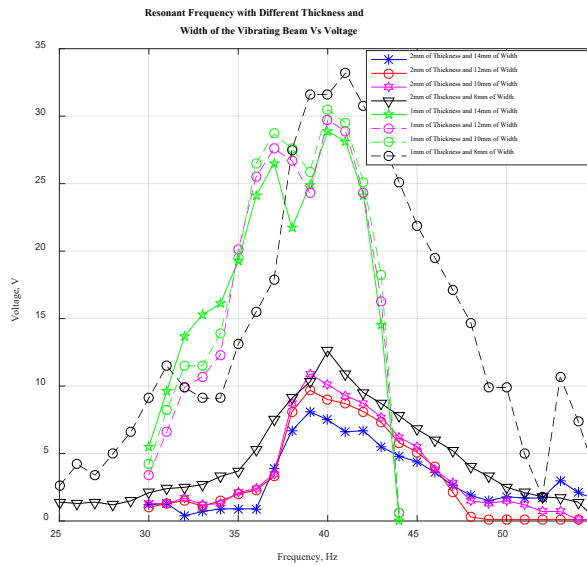


Fig. 10 - Frequency response of the output voltage

An experiment that evaluates the angular acceleration of the beams was first carried out. This was done by employing a weight drop test to the beams. A 7g stainless-steel ball is used in this experiment. Fig. 8 shows the results. This figure shows that the wider the vibrating beam, the lower the angular acceleration for both vibrating beam's thickness. As the angular acceleration can be varied by altering the mass as well as width of the vibrating beam, equation (4) shows the relationship.

$$\alpha = \frac{F}{mr} \quad (4)$$

The mass of the vibrating beam increased when the width of the vibrating beam is wider. Thus, the angular acceleration will be decreased when the mass is increased. Therefore, the inversely proportional relationship of the angular acceleration and the mass is admissible.

Fig. 9 illustrates the relationship between the stiffness and the width of the vibrating beam. It can be confirmed that the wider the vibrating beam, the higher the stiffness of the vibrating beam. The equation of  $F = kx$  shows the relationship of the force and the displacement, where  $F$  is referred to the applied force,  $k$  is stiffness and  $x$  is linear displacement. Hence, the stiffness is inversely proportional to the linear displacement. This is due to the fact that the angular acceleration is directly proportional to the angular displacement and the angular displacement is directly proportional to the linear displacement according to the equation (5).

$$\alpha = \frac{\theta}{t^2} \quad (5)$$

$$\theta = \frac{S}{r}$$

Where,  $\alpha$  is the angular acceleration,  $\theta$  is angular displacement,  $t^2$  is referred to time,  $S$  is linear displacement and  $r$  is referred to the radius of the curvature. Therefore, the higher the angular acceleration is, the higher the angular displacement as well as the linear displacement. This is indicated by results in Figs. 8 and 9.

Next, evaluation on the frequency response of the power generator when changes are made on the vibrating beam's width and thickness is conducted. The width of the vibrating beam is varied from 8mm to 14mm. The thickness and the length are set to 1mm and 80mm, respectively. Proof mass used is 25g and diameter of the plate is 3mm. The resistance of 30k $\Omega$  is connected as the load and 1g of vibration is used as the input. The resulted voltage and power are plotted in Figs. 10 and 11. Fig. 10 presents that the smaller the width of the vibrating beam is, the higher the amplitude of the output voltage. The highest output voltage 33.2V<sub>max</sub> is generated by utilizing the 8mm of width of the vibrating beam. Then, the output voltages are peaked at 30.5V, 29.7V and 28.9V for other vibrating beams. The plotted graph presents that as the frequency increased from 25Hz to 41Hz, the output voltage is increased gradually. Then, the output voltage starts to decline progressively when the frequency is increased from 41Hz to 55Hz for the width of the vibrating beam of 8mm. While for the other vibrating beams, the output voltage is increased slowly when the frequency is increased from 30Hz to 40Hz. After 40Hz, the output voltage is reduced abruptly. The bandwidth of the operating frequency for the 8mm width of vibrating beam is 16Hz wider compared to others. This is due to the anti-resonance of the 8mm vibrating beam is different with the others. Equation (6) describes the relationship of the frequency response and the beam's width. In this equation,  $f$  is frequency,  $f_{impact}$  is the force of impact,  $\Delta L$  is the p-p displacement, and  $m_{eff}$  is the effective mass.

$$f = \pm \sqrt{F_{impact} \left( \frac{2}{\Delta L} \right) \left( \frac{1}{4\pi^2 m_{eff}} \right)} \quad (6)$$

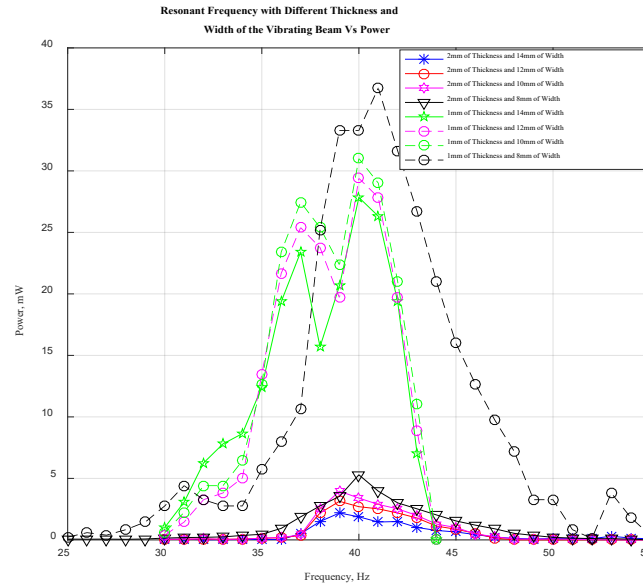


**Fig. 11 - The frequency response of the output power**

Due to  $w \propto m_{eff}$  and  $m_{eff} \propto \frac{1}{f}$ , therefore,  $w \propto \frac{1}{f}$ . Fig. 10 illustrates the range of the operating frequency of

the 2mm thickness of the vibrating beam. The plotted graphs shows that increment in the beam’s width will reduce the output efficiency of the transducer. Equations (4) and (5) can be referred for the relationship of the beam’s width, displacement and stiffness. This is shown in Figs. 8 and 9. As the linear displacement is increased, the applied force of the vibrating beam hits on the piezoelectric disc will be increased according to the equation of  $F = kx$  which is described before. Therefore, the output efficiency of the piezoelectric disc will be improved as well. Furthermore, Fig. 10 displays that decrement of about 64% when the thickness of the vibrating beam is varying from 1mm to 2mm.

According to the equation  $\sigma_b = \frac{3PL}{2wt^2}$  and equation (3), the output voltage is inversely proportional to the thickness of the vibrating beam. The resonant frequency of the piezoelectric for the vibrating beam’s thickness of 1mm is 40Hz. Meanwhile, the resonant frequency of the piezoelectric for the vibrating beam with 2mm of thickness is 39Hz. Same as Fig. 10, Fig. 11 also demonstrates the output power is decreased by 87% when 1mm thickness of the vibrating beam is altered to 2mm of thickness.

Besides that, the frequency responses of the piezoelectric disc are same in pattern with the Fig. 10. This is because  $P = VI$ , amplitude of the output power of the piezoelectric is directly proportional to the output voltage.

#### 4. Conclusion

There are two things that have been discussed in this paper. They are the output efficiency and the frequency response of the power generator as well as the piezoelectric disc. From the experimental results, output efficiency can be increased by introducing the interfaced plate to the configuration of the power generator. Furthermore, it also can be concluded that in order to improve the frequency response of the power generator, the width and the thickness of the vibrating beam need to be adjusted properly.

#### Acknowledgement

The authors would like to thank Universiti Teknikal Malaysia Melaka (UTeM) for the sponsorship given under research Grant: JURNAL/2019/FKEKK/Q00025.

#### References

- [1] Yan, N. X., Basari, A. A., & Nawir, N. A. A. (2018). Piezoelectric ceramic for energy harvesting system: a review. *Journal of Engineering and Applied Sciences*, 13, 22, 8755-775
- [2] Morel, A., Grézaud, R., Pillonnet, G., Gasnier, P., Despesse, G., & Badel, A. (2016). Active AC/DC control for wideband piezoelectric energy harvesting. *Journal of Physics: Conference Series*, 773, 1, 1-4
- [3] Martinez-Ayuso, G., Friswell, M. I., Adhikari, S., Khodaparast, H. H., & Featherston, C. A. (2017). Energy

- harvesting using porous piezoelectric beam with impacts. *Procedia Eng.*, 199, 3468–3473
- [4] Bai, Y. et al. (2018). Investigation of a cantilever structured piezoelectric energy harvester used for wearable devices with random vibration input. *Mech. Syst. Signal Process.*, 106, 303–318
- [5] Halim, M. A., Khym, S., & Park, J. Y. (2013). Impact based frequency increased piezoelectric vibration energy harvester for human motion related environments. *The 8th Annual IEEE International Conference on Nano/Micro Engineered and Molecular Systems*, 949–952
- [6] Viswanath, A. K., & Srikanth, K. (2017). State of art: Piezoelectric Vibration Energy Harvesters. *Mater. Today Proc.*, 4, 2, 1091–1098
- [7] Ali, N. M., Mustapha, A. A., & Leong, K. S. (2013). Investigation of hybrid energy harvesting circuits using piezoelectric and electromagnetic mechanisms. *IEEE Student Conference on Research and Development*, 564–568
- [8] Palosaari, J., Leinonen, M., Juuti, J., & Jantunen, H. (2018). The effects of substrate layer thickness on piezoelectric vibration energy harvesting with a bimorph type cantilever. *Mech. Syst. Signal Process.*, 106, 114–118
- [9] Jing, B. Y., & Leong, K. S. (2016). Parametric Studies on Resonance Frequency Variation for Piezoelectric Energy Harvesting With Varying Proof Mass and Cantilever Length. *Journal of Telecommunication, Electronic and Computer Engineering*, 8, 5, 119–123
- [10] Alame, A. H., Gratuze, M., Elsayed, M. Y., & Nabki, F. (2018). Effects of Proof Mass Geometry on Piezoelectric Vibration Energy Harvesters. *Sensors*, 18, 5
- [11] Bong, Y. J., & Leong, K. S. Leong. (2017). Broadband Energy Harvesting using Multi-Cantilever based Piezoelectric. *J. Telecommun. Electron. Comput. Eng.*, 9, 3, 111–116
- [12] Wang, Y., He, H., & Xu, R. (2015). An analytical model for a piezoelectric vibration energy harvester with resonance frequency tunability. *Adv. Mech. Eng.*, 7, 6
- [13] Jackson, N., Stam, F., Olszewski, O. Z., Houlihan, R., & Mathewson, A. (2015). Broadening the Bandwidth of Piezoelectric Energy Harvesters Using Liquid Filled Mass. *Procedia Eng.*, 120, Supplement C, 328–332
- [14] Jing, B. Y., & Leong, K. S. (2016). Demonstration of piezoelectric cantilever arrays for broadband vibration harvesting. *IEEE International Conference on Power and Energy (PECon)*, 814–817
- [15] Uddin, M. N., Islam, M. S., Sampe, J., Wahab, S. A., & Ali, S. H. M. Ali. (2016). Proof mass effect on piezoelectric cantilever beam for vibrational energy harvesting using Finite Element Method. *International Conference on Radar, Antenna, Microwave, Electronics, and Telecommunications (ICRAMET)*, 17–21
- [16] Xie, X. D., Carpinteri, A., & Wang, Q. (2017). A theoretical model for a piezoelectric energy harvester with a tapered shape. *Eng. Struct.*, 144, Supplement C, 19–25
- [17] Xue, H., Hu, Y., & Wang, Q. (2008). Broadband piezoelectric energy harvesting devices using multiple bimorphs with different operating frequencies. *IEEE Trans. Ultrason. Ferroelectr. Freq. Control*, 55, 9, 2104–2108
- [18] Kumar, T., Kumar, R., & Chauhan, V. S. (2015). Design and finite element analysis of varying width piezoelectric cantilever beam to harvest energy. *International Conference on Energy, Power and Environment: Towards Sustainable Growth (ICEPE)*, 1–6
- [19] Yang, Z., Wang, Y. Q., Zuo, L., & Zu, J. (2017). Introducing arc-shaped piezoelectric elements into energy harvesters. *Energy Convers. Manag.*, 148, 260–266
- [20] Basari, A. A., et al. (2014). Shape effect of piezoelectric energy harvester on vibration power generation. *J. Power Energy Eng.*, 2014, 2, 117–124
- [21] Choi, K. N., & Rho, H. H. (2015). Continuous energy harvesting method using piezoelectric element. *IEEE 2nd International Future Energy Electronics Conference (IFEEC)*, 1–4
- [22] Yan, N. X., Basari, A. A., Leong, K. S., Nawir, N. A. A., & Hashimoto, S. (2018). Investigation and experimental verification of the effectiveness of the interfaced plate parameters on impact-based piezoelectric energy harvester. *Ceramics International*, 44, 15, 17724–17734
- [23] Basari, A. A., et al. (2015). Evaluation on mechanical impact parameters in piezoelectric power generation. *10<sup>th</sup> Asian Society Control Conference (ASCC)*, 1–6
- [24] Abdal-Kadhim, A. M., & Leong, K. S. (2016). Piezoelectric impact-driven energy harvester. *IEEE International Conference on Power and Energy (PECon)*, 407–411
- [25] Abdal-Kadhim, A. M., & Leong, K. S. (2017). Piezoelectric Pre-Stressed Bending Mechanism for Impact-Driven Energy Harvester. *IOP Conf. Ser. Mater. Sci. Eng.*, 210, 1, 12037
- [26] Halim, M. A., Cho, H. O., & Park, J. Y. (2015). A handy motion driven, frequency up-converting piezoelectric energy harvester using flexible base for wearable sensors applications. *SENSORS*, 1–4
- [27] Ju, S., & Ji, C. H. (2015). Indirect impact based piezoelectric energy harvester for low frequency vibration. *18th International Conference on Solid-State Sensors, Actuators and Microsystems (TRANSDUCERS)*, 1913–1916
- [28] Janphuang, P., Lockhart, R. A., Isarakorn, D., Henein, S., Briand, D., & De Rooij, N. F. (2015). Harvesting energy from a rotating gear using an AFM-like MEMS piezoelectric frequency up-converting energy harvester.

- J. Microelectromechanical Syst., 24, 3, 742–754
- [29] Minh, V. L., Hara, M., & Kuwano, H. (2015). Lead-Free (K,Na)NbO<sub>3</sub> Impact-Induced-Oscillation Microenergy Harvester. J. Microelectromechanical Syst., 24, 6, 1887–1895
- [30] Basari, A. A., Hashimoto, S., Homma, B., Okada, H., Okuno, H., & Kumagai, S. (2016). Design and optimization of a wideband impact mode piezoelectric power generator. Ceramics International, 42, 6, 6962–6968
- [31] Hashimoto, S., et al. (2016). Evaluation of impact mode-based piezoelectric power generator, IEEE 11th Conference on Industrial Electronics and Applications (ICIEA), 1131–1134